Characterization of Single-Cell Electroporation by Using Patch-Clamp and Fluorescence Microscopy

Frida Ryttsén,* Cecilia Farre,* Carrie Brennan,† Stephen G. Weber,† Kerstin Nolkrantz,* Kent Jardemark,* Daniel T. Chiu,* and Owe Orwar*

*Department of Chemistry, Göteborg University, Göteborg SE-412 96, Sweden and †Department of Chemistry, University of Pittsburgh, Pittsburgh, Pennsylvania, 15260 USA

ABSTRACT Electroporation of single NG108-15 cells with carbon-fiber microelectrodes was characterized by patch-clamp recordings and fluorescence microscopy. To minimize adverse capacitive charging effects, the patch-clamp pipette was sealed on the cell at a 90° angle with respect to the microelectrodes where the applied potential reaches a minimum. From transmembrane current responses, we determined the electric field strengths necessary for ion-permeable pore formation and investigated the kinetics of pore opening and closing as well as pore open times. From both patch-clamp and fluorescence microscopy experiments, the threshold transmembrane potentials for dielectric breakdown of NG108-15 cells, using 1-ms rectangular waveform pulses, was ~250 mV. The electroporation pulse preceded pore formation, and analyte entry into the cells was dictated by concentration, and membrane resting potential driving forces. By stepwise moving a cell out of the focused field while measuring the transmembrane current response during a supramaximal pulse, we show that cells at a distance of ~30 μm from the focused field were not permeabilized.

INTRODUCTION

During the last two decades, there has been a tremendous growth in the number of experimental methods available for the biochemical and biophysical investigations of single cells. Such methods include 1) patch-clamp techniques for measuring transmembrane currents through a single ion channel (Hamill et al., 1981), 2) scanning confocal and multiphoton microscopy for imaging and localizing bioactive components in single cells and single organelles (Maiti et al., 1997), 3) near-field optical probes for measuring pH in the cell interior (Song et al., 1997), 4) ultramicroelectrodes for monitoring the release of single catechol- and indol-amine-containing vesicles (Chow et al., 1992, Wightman et al., 1991), and 5) optical trapping and capillary electrophoresis separations for analyzing the chemical composition of individual secretory vesicles (Chiu et al., 1998).

Although numerous high-resolution techniques exist to detect, image, and analyze the contents of single cells and subcellular organelles, few methods exist to control and manipulate the biochemical nature of these compartments. Most compounds of biological and medical interest are polar and therefore unable to cross cell membranes. Examples of such compounds are dyes, drugs, DNA, RNA, proteins, peptides, and amino acids. At present, it is extremely difficult, for example, to label an individual cell in a cell culture with a dye, or transfect it with a gene without labeling or transfecting its adjacent neighbor.

Electroporation is a frequently applied technique for introduction of charged or polar molecules into intracellular domains of a plurality of cells. The application of an external electric field across artificial or biological phospholipid bilayer membranes results in increased permeability and conductance of the membrane (Zimmermann, 1982, Zimmermann et al., 1974).

The membrane voltage, V_m, at different locations of a spherical cell membrane in a homogeneous electric field for duration t, can be calculated from

$$V_m = 1.5 r_c E \cos\alpha[1 - \exp(-t/\tau_m)], \quad (1)$$

where E is the electric field strength, r_c is the radius of the cell, α is the angle in relation to the direction of the electric field, and

$$\tau_m = r_c C_m((R_{int} + R_{ext})/2) \quad (2)$$

is the membrane relaxation time. C_m is the membrane capacitance, and R_{int} and R_{ext} are the specific resistivities of the intracellular and extracellular media. When electroporation is performed by using inhomogeneous electric fields as in the present study, the electric field gradient has to be taken into account for estimates of V_m.

The applied electric field will generate large depolarizing and hyperpolarizing transmembrane potentials at the cathode- and anode-facing poles of the cell, respectively. When the membrane potential reaches a critical value, typically 0.2–1.5 V for mammalian cells, dielectric membrane breakdown will occur, which results in pore formation. Pore density will follow the V_m-gradient, and is highest at the polarized (electrode-facing) ends of a cell. During the effective pore-open time, cell-impermeant solutes added to the extracellular medium can enter the cell interior (Weaver, 1993).

The conductance caused by dielectric breakdown of membranes is proportional to the amplitude and duration of the electric field (Neumann et al., 1998). Kinosita and Tsong, (1977a,b) reported an effective pore diameter of 1 nm for human erythrocyte membranes and concluded that the size of the pores was determined by field strength, pulse duration, pH, and

Received for publication 13 March 2000 and in final form 10 July 2000.

Address reprint requests to Owe Orwar, Department of Chemistry, Göteborg University, Göteborg SE-412 96, Sweden. Tel.: +46-31-772-2778; Fax: +46-31-772-2785; E-mail: orwar@amc.chalmers.se.

Dr. Kent Jardemark's present address is Department of Psychiatry and Behavioral Science, State University of New York at Stony Brook, Stony Brook, NY 11794-8790.

Dr. Daniel T. Chiu's present address is Department of Chemistry and Chemical Biology, Harvard University, Cambridge, MA 02138.

© 2000 by the Biophysical Society

0006-3495/00/10/1993/09 $2.00

ionic strength of the suspending medium. Chang and Reese, (1990) observed pores with diameters between 6 and 240 nm in human erythrocyte membranes by rapid-freeze fracture electron microscopy. In charge-pulse studies on irreversible breakdown of planar lipid bilayers, pores with diameters up to 400 μm were observed (Wilhelm et al., 1993).

The duration, strength, and wave function of the applied electric pulse also determines whether the electropermeabilization of the membrane will be reversible or irreversible or of a punch-through type (Weaver, 1993). Reversible dielectric breakdown occurs when high-voltage, short-duration pulses are applied, wherein the pores are formed and resealed within fractions of a second (Benz and Zimmermann, 1980; Weaver, 1993). Resealing of the membrane is a two-step process. Within a few milliseconds after the pulse, the membrane conductance is significantly decreased although the number of pores remain constant, indicating that the radii of the pores has decreased. The decrease in the number of pores is a much slower process because of an energy barrier that prevents closure. The disappearance of pores takes seconds (Glaser et al., 1988). Also, formation of metastable pores after reversible dielectric breakdown with resealing times from seconds to hours has been observed (Kinosita and Tsong, 1977a; Chernomordik et al., 1987; Lopez et al., 1988).

In addition to bulk electroporation methods, instrumentation has been developed that can be used for electroporation of a small number of cells in suspension (Chang, 1989; Kinosita and Tsong, 1979; Marszalek et al., 1997) and for a small number of adherent cells grown on a substratum (Teruel and Meyer, 1997; Zheng and Chang, 1991). These electroporation devices create homogeneous electric fields across fixed distances of 0.1–5 mm, several times larger than the size of a single mammalian cell.

We recently reported on a highly spatially resolved electroporation technique, miniaturized to perform experiments at the single-cell and subcellular level (Lundqvist et al., 1998). The electrodes are of smaller dimension than a single cell and are controlled individually with high-graduation micropositioners, which enables precise electrode alignment in all three directions. This capability makes possible the electroporation or electrofusion of a single selected cell in a confluent cell culture (Lundqvist et al., 1998; Strömberg et al., 2000). In addition to the high spatial resolution achieved by using ultramicroelectrodes, this experimental arrangement avoids the use of high-voltage pulse generators and complicated microchamber mounts. In contrast to microinjection techniques for single cells and single nuclei (Capecchi, 1980), the present technique can be applied to biological containers of sub-femtoliter (10^{-15} l) volumes, that are less than a few micrometers in diameter. Electroporation has other advantages over microinjection techniques in that it can be extremely fast, and well-timed (Kinosita et al., 1988; Hibino et al., 1991), which is of importance in studying fast reaction phenomena.

This paper describes our studies on the mechanisms of microelectrode electroporation using patch-clamp and fluorescence microscopy. Because most characterization of electroporation has been performed in batch mode with homogeneous electric fields, no in-depth characterization is available for single-cell electroporation using inhomogeneous electric fields. This characterization is necessary for finding optimal protocols for the loading of single cells. In addition, a patch-clamp electroporation method that enables probing of membrane properties during and after exposure of a single cell to a DC electric field is a valuable tool for studying membrane dynamics. Patch-clamp recordings have previously been demonstrated as a powerful method to monitor dielectric membrane breakdown in biological and synthetic membranes under the influence of a homogeneous electric field (O'Neill and Tung, 1991; Owen and Piotrowski, 1987; Sharma et al., 1996). NG108-15 cells were patch clamped in the whole-cell configuration as described elsewhere (Hamill et al., 1981), and the electroporation electrodes were positioned on opposite sides of the cell. The spatial distribution of the electric field was characterized by stepwise moving the cell out of the focused field. The potential needed for membrane breakdown was determined by applying 1-ms rectangular waveform pulse sequences of increasing voltages. The potential drop due to the solution resistance was determined in separate experiments to estimate the effective electric field strength. Furthermore, from the patch-clamp recordings, pore opening and resealing kinetics, and pore open times were determined.

MATERIALS AND METHODS

NG108-15 cells were grown in Dulbecco's minimum essential medium supplemented with 10% calf serum and 1% antibiotics at 37°C in a humidified 5% CO_2, 95% air atmosphere. For patch-clamp experiments, the culture medium was replaced by a HEPES buffer (140 mM NaCl, 10 mM HEPES, 10 mM D-glucose, 5 mM KCl, 1 mM $CaCl_2$, 1 mM $MgCl_2$, and pH was adjusted to 7.4 with NaOH). The cells were mechanically removed from the petri dish in which they were cultured, and then separated from each other in a Pasteur pipette by shear forces and plated onto #1 circular coverslips just before experiments. The cell dishes were mounted on an inverted microscope (Leica DM IRB, Wetzlar, Germany) equipped with a Leica Fluotar 40× objective. All experiments were performed at room temperature.

Before experiments, cells were left to rest for 10–15 min. Recordings were performed in the whole-cell configuration, and the inside of the cell membrane was clamped at −50 mV with respect to the grounded bath. Data were stored on videotape (digitized at 20 kHz) and were analyzed later (sample frequency 2 kHz, filter frequency 1 kHz). The time delay between the electroporation pulse and transmembrane current events, the amplitude of the transmembrane current, and the time needed for complete recovery were obtained from the traces. The high level of noise in the traces was caused by laser flickering. The pipette solution contained 100 mM KCl, 2 mM $MgCl_2$, 1 mM $CaCl_2$, 11 mM EGTA, and 10 mM HEPES (pH was adjusted to 7.2 with KOH).

For electroporation, we used 5-μm-outer-diameter carbon fiber microelectrodes (Pro CFE, Dagan Corporation, Minneapolis, MN) controlled by high-graduation micromanipulators (Narishige MWH-3, Tokyo, Japan). The carbon fibers were enclosed in a plastic tip filled with 3 M KCl that was in contact with a silver wire connected to the voltage-pulse generator (Digitimer Stimulator DS9A, Welwyn Garden City, U.K.). To study the potential needed for dielectric membrane breakdown, the two electrode tips were positioned 2–5 μm from the outer cell surface at an angle of 0–20°, and 160–180° with respect to the object plane, and 90° with respect to the patch pipette (Fig. 1). Cells were electropermeabilized by application of monophasic 1-ms rectangular DC voltage pulses of increasing field strengths from 1.1 to 8.1 kV/cm (not corrected for voltage drop due to solution resistance). By studying the current responses from the cells, the potential needed to cause pore formation in the plasma membrane could be

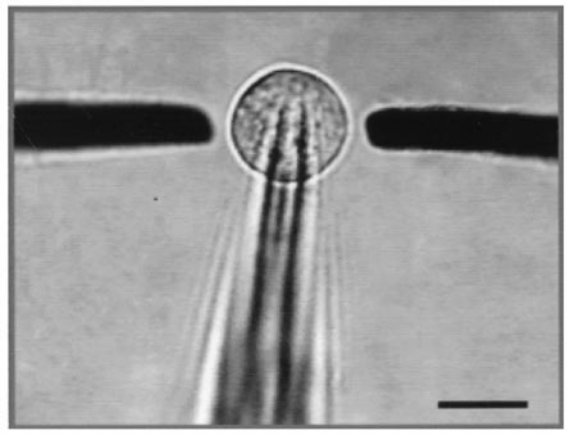

FIGURE 1 Photomicrograph showing a patch-clamped NG108-15 cell, flanked by 5-μm-outer diameter carbon fiber ultramicroelectrodes. Scale-bar = 10 μm.

determined. Figure 2 shows schematically how electroporation and patch clamp were performed on a single cell. The spatial distribution of the electric field was studied by stepwise withdrawal of a cell out of the focused field in steps of 2, 5, 8, 10, 11, 12, and 27 μm, and measuring the current response while applying a supramaximal pulse of 3.7 kV/cm. Permeabilization of the membrane and closure of pores could also be determined from the current responses during and after the pulse in the patch clamp experiments.

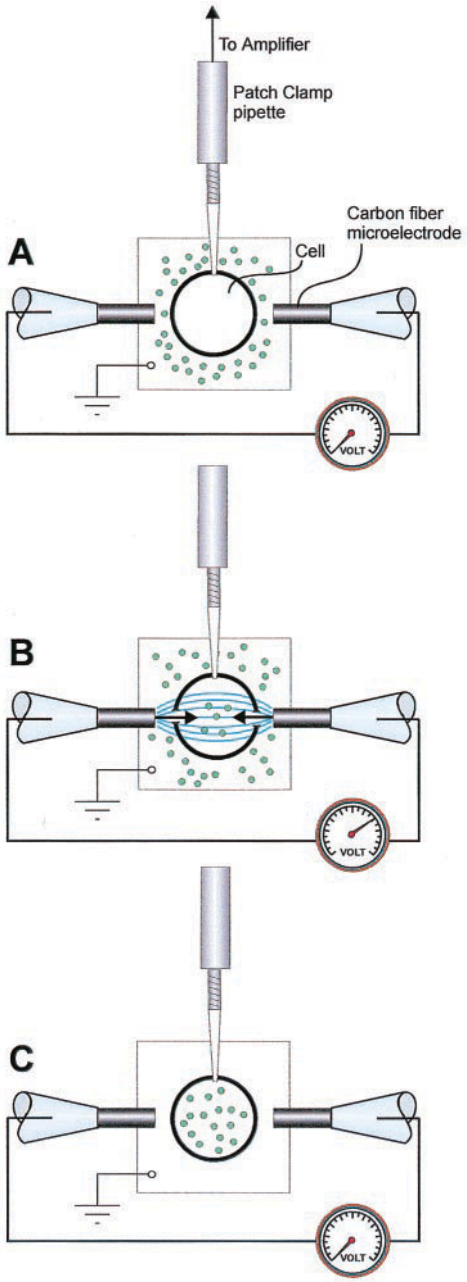

FIGURE 2 Schematic drawing of the experimental setup. (*A*) A patch-clamped cell in buffer solution containing the solutes to be introduced into the cell. The electrodes are positioned in a linear opposing fashion across the cell, at a 90° angle with respect to the patch pipette. (*B*) A pulse is applied, and solutes can diffuse into the cell after pores are formed. (*C*) After the pulse, the extracellular medium is exchanged, and the solutes are present only in the electroporated cell.

For fluorescence experiments, cells were grown for 1–2 days, and the culture medium was replaced with an intracellular buffer consisting of 135 mM KCl, 5 mM NaCl, 20 mM HEPES, 1.5 mM $MgCl_2$, 10 mM glucose, and 5 μM fluorescein, pH was adjusted to 7.4 with NaOH. The cells were electroporated with ten pulses of 1-ms duration and electric field strengths of 1.3–6.5 kV/cm (values not corrected for potential drop), washed several times so no extracellular fluorescein remained in the buffer, and dye trapped inside the cells was detected. For excitation of fluorescein, an Ar^+-laser (Spectra-Physics 2025–05, 488 nm), a 488 nm-line interference filter, a spinning disk to break the coherence, an inverted microscope (DMIRB, Leica) equipped with a 40× objective to focus and collect the laser light, and a fluorescein filter cube (I-3, Leica) were used. Images were recorded with a 3-chip color CCD-camera (C6157, Hamamatsu, Kista, Sweden) and stored at 25 Hz collection rate on a Super VHS (S-VHS AG-5700, Panasonic, Stockholm, Sweden). Fluorescence intensity was measured using an image processor (Hamamatsu). The CCD images were digitized from tape and processed for presentation.

Solution resistance studies were performed using a waveform generator (Model DS345, Stanford Research Systems, Sunnyvale, CA) to apply pulses, and a digital oscilloscope (Model 9410, Lecroy, Chestnut Ridge, NY) with GPIB connection for computerized data collection. The current signal from the electrodes was amplified using a home-built current-to-voltage converter before going into the oscilloscope. Applied pulses were 1-ms long, with a rest period of 1.63 s between pulses. All experiments were performed in HEPES buffer solution (140 mM NaCl, 10 mM HEPES, 10 mM D-glucose, 5 mM KCl, 1 mM $CaCl_2$, 1 mM $MgCl_2$, and pH adjusted to 7.4 using NaOH). Commercial microelectrodes (Dagan Corp., Minneapolis, MN) were positioned using micromanipulators (Narishige Co. Ltd., Tokyo, Japan), and viewed under a stereo microscope (Fisher Scientific, Blawnox, PA).

Chemicals

HEPES (>99%), sodium chloride, potassium chloride, and sodium hydroxide (all suprapur), calcium chloride, magnesium dichloride, D-glucose and EGTA (Titriplex VI) (all pro analysis) were purchased from Merck (Darmstadt, Germany). Fluorescein (GC-grade) was obtained from Sigma (St. Louis, MO). Deionized water from a Milli-Q system (Millipore, Bedford, MA) was used.

RESULTS

Electrochemical reactions and spatial electric field focusing

The strength of the electric field over the cell in our setup is not equal to the applied electric field strength because of initiation of electrode reactions and the formation of an electric double layer at the surface of the electrodes. The determination of the potential gradient experienced by the cells has been investigated by Weaver and co-workers (Bliss et al., 1988; Gift and Weaver, 1995; Pliquett and Weaver, 1996; Pliquett et al., 1995; Pliquett et al., 1996; Prausnitz et al., 1993; Weaver and Chizmadzhev, 1996). In normal electroporation experiments, there are several concerns, including the dynamics of the voltage distribution and the fraction of the applied voltage that ends up across the cell (Pliquett et al., 1996). In the current experimental setup, we are also concerned with these issues. The problem of the amount of the applied voltage appearing across the solution is particularly important for these microelectrode

systems because the voltage drop at the electrode–solution interface is significant in comparison with the applied voltage.

For small applied voltages (<2 V), the potential gradient in solution is very small at long times (>100 μs). At short times, the convolution of the instrumental rise time and the electrode/electrolyte charging time gives rise to a peak-shaped field-versus-time curve. The maximum magnitude of the applied voltage in solution can be calculated by convoluting exponential functions for the instrument rise time and the charging time. For our particular case, with an instrument rise time of 8 μs, and a charging time in the range 20–40 μs, the maximum amplitude is 15–18% of the applied pulse amplitude. This maximum occurs ~10–15 μs after application of the pulse. For example, a 1.0-V pulse would result in a maximum of about a 150-mV potential difference between the electrodes, occurring ~10–15 μs after application of the pulse. After ~50–75 μs, the potential drop is effectively zero because all of the applied voltage appears at the electrode–solution interfaces.

We hypothesize that, at high voltages, the interfacial impedance becomes negligible, and the current that passes between the microelectrodes is limited by the solution conductance. To determine the potential drop across the solution, 1-ms pulses were applied across pairs of carbon fiber microelectrodes separated by 5–50 μm in a HEPES buffer solution. The solution resistance was calculated by plotting the current at the end of the pulse as a function of applied potential between 9 and 10 V. Resistance was determined by linear regression (the inverse of the conductance, see Fig. 3). The fact that the current is linearly related to the applied voltage supports the idea that the medium is resistive. This process was repeated for each electrode separation distance. The solution resistance was found to be 27 ± 3 kΩ for distances of 10 μm and greater. The constant value of the calculated resistance reflects the nature of the field created in solution. The field lines converge onto the electrodes, so most of the potential drop occurs near the electrodes. Solution potential drops were calculated by multiplying the current at 1 ms by the calculated resistance value. The potential drop across the solution increases considerably with increasing applied potential (see Fig. 4), but only slightly with increasing electrode separation.

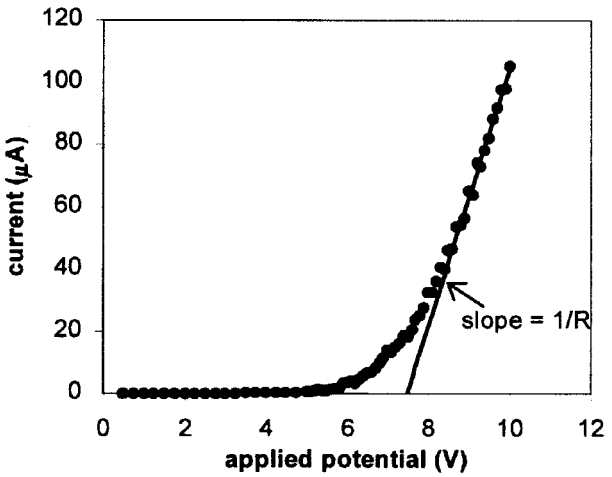

FIGURE 3 A plot of current versus applied potential. Current values were those at the end of a 1-ms pulse. Solution resistance was the inverse of the slope, determined by taking a linear regression of current values between 9 and 10 V. Applied potentials ranged from 0.5 to 5 V at 0.25-V intervals, and from 5 to 10 V at 0.1-V intervals; electrode separation was 25 μm.

In general, solution-resistance (conductance) measurements usually are not done at DC because of the dual problems of electrolysis and double-layer potential drop. With microelectrodes, however, AC measurements cannot be used because of their small capacitance. If the frequency used is high enough for the current to "see" a low impedance in the double layer, then it is too high for commonly used instrumentation. Also, we are not able to use a 4-probe type measurement (Pliquett et al., 1996) in which a pair of measuring electrodes was placed between the two potential application electrodes, because of the small dimensions of our system. Thus, we are forced to use the alternative approach described above.

Membrane potentials reported in this article will be given as calculated from Eq. 1 without voltage-drop correction for electrode reactions and solution resistance. Because Eq. 1 is written for homogeneous electric fields, this only gives an estimate of the magnitude of the fields in our system. Field strengths are reported as applied potential with respect to electrode separation.

The spatial distribution of the electric field was studied by stepwise withdrawal of patch-clamped cells out of the center of the electrodes. By measuring transmembrane currents at each position, at a constant applied voltage pulse, the effect of the field on the cell could be determined. Cells were moved out of the field in steps of 2, 5, 8, 10, 11, 12, and 27 μm, and, for each movement, a supramaximal pulse of 3.7 kV/cm and 1-ms duration was applied. Figure 5 shows that, at a distance of 27 μm from the field focus, the current response was only −25 pA, which is 16% of the current response at the field focus. When patch-clamped cells were positioned 40 and 67 μm from the field focus, extremely high field strengths were needed to obtain a transmembrane current response, 5.6 kV/cm and 6.7 kV/cm, respectively.

Threshold membrane potential for dielectric breakdown in NG108-15 cells

From patch-clamp measurements, the transmembrane threshold potential for pore formation of NG108-15 cells was determined to be ~2.5 V. When corrected for the voltage drop at the double layer, this corresponds to ~250

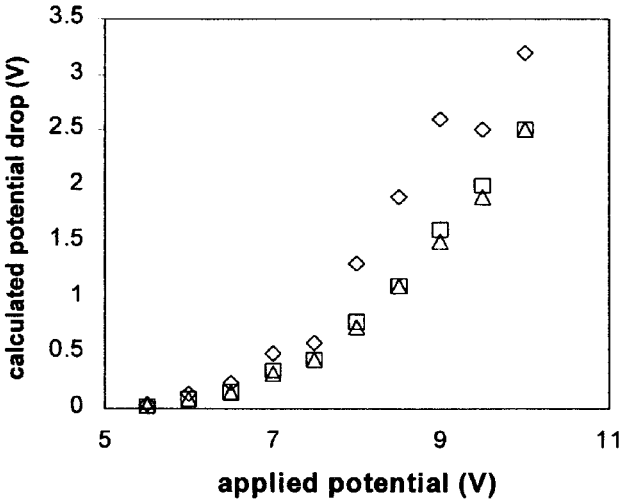

FIGURE 4 A plot of the solution potential drop calculated using the estimated resistance and experimental currents (at the end of 1-ms pulses) for electrode separations of 5 μm (*diamonds*), 25 μm (*squares*), and 50 μm (*triangles*).

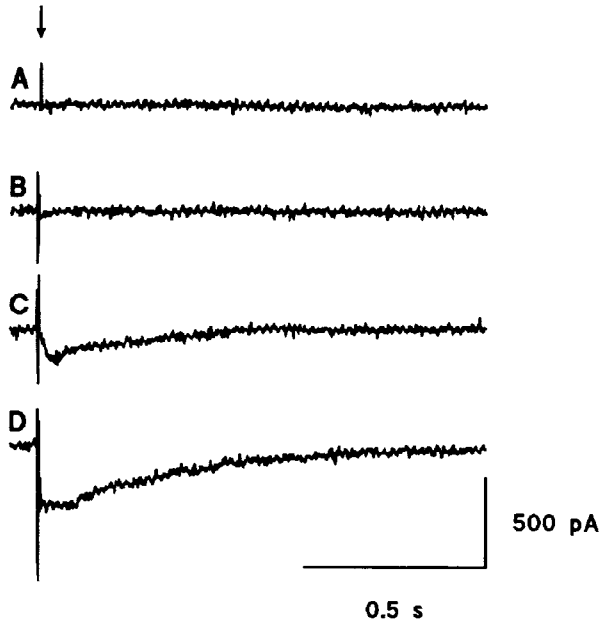

FIGURE 6 Patch-clamp traces recorded from a NG108-15 cell (holding potential, −50 mV) electroporated at (*A*) 2.7, (*B*) 3.2, (*C*) 3.8, and (*D*) 4.3 kV/cm. Maximum current responses were 0, −35, −190, −330 pA, respectively, indicating an increased number of pores formed or a higher degree of pore expansion at higher fields. The arrow indicates application of the voltage pulse.

mV, which is in good agreement with previous reports (Teissié and Rols, 1993; Teissié and Tsong, 1981). Membrane-potential values higher than ~4 V resulted in irreversible membrane breakdown, and the cells did not recover. Figure 6 shows transmembrane current responses from a cell electroporated with increasing voltage. Dielectric membrane breakdown was observed from ~2.5 V, resulting in currents in the range of −30 to −330 pA. Results presented in Table 1 indicate that membrane ion-

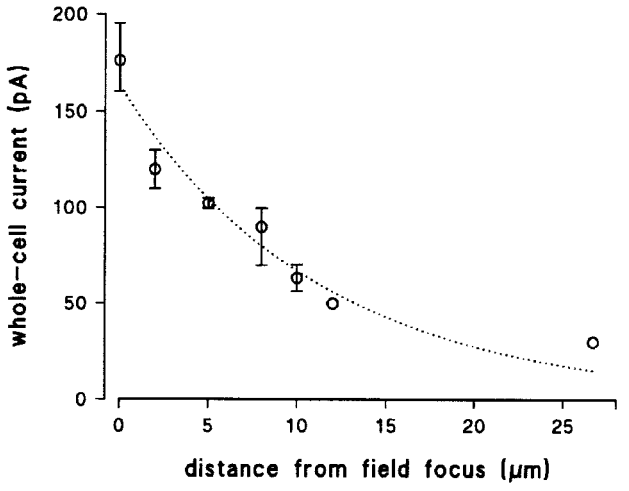

FIGURE 5 Dependence of maximum transmembrane current responses (mean ± S.D., $N = 16$) on the distance from the field focus. As a cell is moved out of the field, the influence of the field diminishes, and at distances farther than ~30 μm from the electric field focus, almost no permeation of the cell occurs. Voltage pulses of the same amplitude were applied as a clamped (−50 mV) NG108-15 cell was positioned at different distances from the field focus.

permeability is lower for potentials near the threshold value than for higher potentials. The high conductance state is also more prolonged for higher voltages than for threshold potentials. An increase of the field strength can also result in morphological changes in the cells, such as chromatin condensation, swelling of organelles, and retraction of processes to the cell body.

The results obtained in the fluorescence experiments using fluorescein (dianion, MW 376.3) as a marker are in agreement with the patch clamp data. Figure 7 shows fluorescence intensity as a function of applied voltage, and Fig. 8 shows fluorescence and brightfield micrographs of the electroporated cells. The threshold membrane potential required for a detectable difference in fluorescence intensity, obtained by comparing control and electroporated cells, was 3.0 V, and the fluorescence intensity increased with higher electric field strengths. Figure 8 also shows that cells electroporated at supramaximal field strengths had a swollen and granulated appearance.

Kinetics of pore-expansion and resealing

During the 1-ms pulse, a peak response is typically seen due to capacitive charging of the patch pipette, and the response from the electroporated membrane appears as an increase in the membrane conductance immediately or a few milliseconds after the pulse. The time for expansion/evolution of the

TABLE 1 Patch-clamp data of electroporated NG108-15 cells

Membrane Potential (V)	Transmembrane Current (pA)	Pore Expansion/Evolution Rate (pA/ms)	Pore Expansion/Evolution Time (ms)	Time at Maximum Current (ms)	Recovery Time (ms)
2.5	−32	ND	3	6	10
	−48	ND	0	10	20
	−50	ND	6	9	17
	−30	ND	1–2	9	46
Mean ± S.D.	−40.0 ± 10.5	ND	2.6 ± 2.6	8.5 ± 1.7	23.4 ± 15.5
3.0	−165	−3.60	33	51	329
	−185	−4.50	37	51	505
	−190	−6.10	27	31	449
	−170	−7.27	19	27	558
Mean ± S.D.	−177.5 ± 11.9	−5.37 ± 1.64	29 ± 7.8	40.0 ± 12.8	460.3 ± 98.2
3.7	−160	−3.08	40	65	620
	−260	−4.14	50	51	368
	−175	−3.96	22	65	385
	−170	−5.71	23	82	380
	−175	−6.09	29	104	551
	−165	−5.48	29	64	500
Mean ± S.D.	−184.2 ± 37.6	−4.74 ± 1.19	32 ± 10.8	71.8 ± 18.6	467.3 ± 105.5

ND = not determined.

pores ranges between 0 and 50 ms (Table 1) at a rate of 3.1–7.3 pA/ms. The high-conductance state of the membrane lasted for 6–104 ms. Recovery times from high-conductance states ranged from 10 to 620 ms. Cells did occasionally have recovery times of seconds to minutes. These cells usually recovered from the high-conductance state within 500 ms, but there seemed to be a low-conductance state stable for longer times. These long time scales are in accordance with previous reports where pores were shown to be stable over very long times, minutes to hours (Chang and Reese, 1990; Chernomordik et al., 1987; Lopez et al., 1988; Kinosita and Tsong, 1977a).

The rate of increase in transmembrane currents was estimated to be −3.1 to −6.1 pA/ms using linear regression.

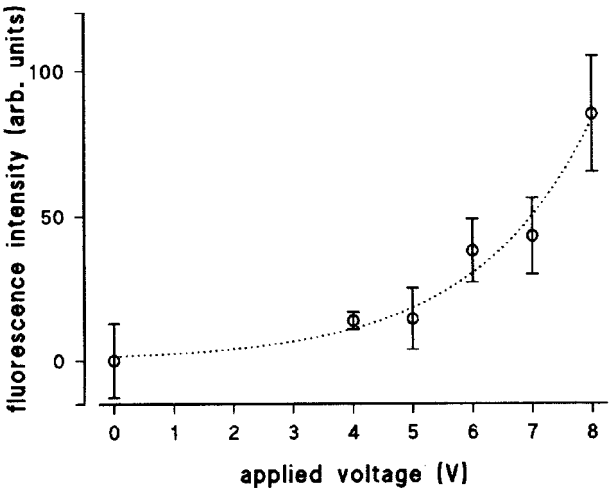

FIGURE 7 A plot of fluorescence intensity (mean ± S.D., $N = 69$) of electroporated cells as a function of applied potential. The electroporation buffer contained 5 μM fluorescein. After electroporation, the extracellular fluorescein was removed and the fluorescence intensity was measured. An applied voltage of 4 and 5 V yielded a slightly higher fluorescence intensity than for control cells. As the applied potentials were increased, the fluorescence intensity increased because either more pores were formed or pore radii expanded and more fluorescein was allowed to diffuse into the cells.

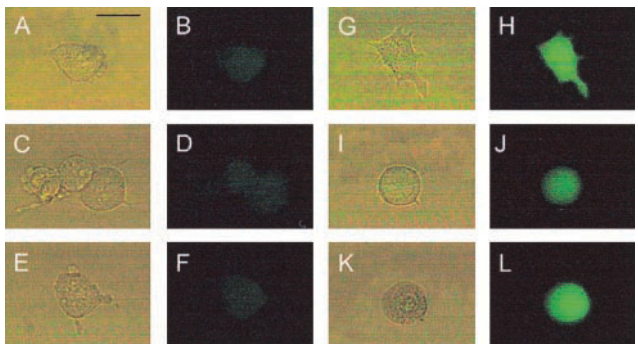

FIGURE 8 Brightfield and fluorescence photomicrographs of control cells (*left row*) and electroporated cells (*right row*). Scalebar = 20 μm. All cells were incubated in buffer supplemented with 5 μM fluorescein. (*A-F*) Control cells exhibit weak fluorescence from fluorescein interacting with the outer boundary of the cell membrane. (*G-L*) Cells were electroporated with increasing field strengths starting at the threshold value of (*G*, *H*) ~3.2 kV/cm, (*I*, *J*) ~3.8 kV/cm, and (*K*, *L*) ~4.3 kV/cm. A higher fluorescence intensity from fluorescein internalized in the cytosol is observed when comparing a statistical number of cells electroporated with higher field strengths. In the brightfield images, one can see that the cells are more swollen (*I*) and granulated (*K*) when exposed to higher electric fields.

DISCUSSION

Electroporation of selected single cells and subcellular structures in a culture requires ultrasmall electrodes, which produces inhomogeneous electric fields. By stepwise withdrawal of a patch-clamped cell out of the field focus, we have shown that the electric field is tightly focused, leaving adjacent cells almost unaffected. Cells were unperturbed at a distance of ~30 μm from the center of the field using supramaximal stimulation. At longer distances from the center of the focused field, 40 and 67 μm, extremely large field strengths were required, 5.6 and 6.5 kV/cm, respectively, for detecting a current response. Such field strengths would cause immediate cell death if the applied electric fields were homogeneous.

The critical field strength for producing a detectable current response is approximately 3.2 kV/cm, which corresponds to a transmembrane potential of ~2.5 V. When the cell membrane is permeabilized through electroporation, transmembrane currents of −35 to −330 pA were observed. Application of field strengths larger than the threshold value caused transmembrane currents of increased magnitudes. Possibly the number of pores increases with increasing applied field strength. Alternatively, the same number of pores are created but expand in size when a higher electric field is applied. Wilhelm et al., (1993) argued that the magnitude of the applied field does not affect the conductance resulting from pore formation. Rather, pore formation is a chaotic event where the probable number of pores is dependent upon applied voltage. What happens to the pores formed is solely determined by the properties of the membrane. In our study, we cannot determine what process caused larger transmembrane currents, but it is evident that, when potentials higher than the threshold value were applied, transmembrane currents increased in magnitude. Well above the threshold potential, the magnitude of the current did not change significantly with increased potential.

Upon repeated electroporation of one cell with the same magnitude of the electric field, the resulting transmembrane current diminished with each subsequent pulse. Chernomordik et al., (1987) reported this effect for low-amplitude pulses, and the opposite effect for high-amplitude and long-duration pulses, that is, the breakdown current becomes higher for each pulse, and the membrane loses its ability to reseal.

In our fluorescence data, the trend is similar, as described above. Below the threshold value, no dye enters the cell. At ~3.0 V, pores are formed, which allows for entry of the dye into the cell; higher transmembrane potentials caused a corresponding increase in fluorescence intensity. The similarity of the curves in Fig. 4 and Fig. 7 shows that the fluorescence response from cells electroporated with increasing field strength in presence of fluorescein is proportional to the voltage drop in the solution.

In the patch-clamp experiments, the cells were lifted up in the electroporation media by the patch pipette, whereas, in the fluorescence experiments, the cells were adherent to the substratum during electroporation. This fact might have contributed to the observed difference in breakdown potential in these two experiments. The threshold potential could also be higher in the fluorescence experiments because they were less sensitive than the patch-clamp recordings.

Typically, pore formation or expansion was observed within a few milliseconds after pulse application. In some experiments, however, a delay of up to 30 ms was observed. This delay is probably caused by the time it takes for the pores to expand to a size sufficient for ions to pass. This time delay is consistent with previously reported data. Chang and Reese (1990) could detect volcano-shaped pores after 3 ms. In their report, pore expansion occurred within 40–120 ms, which is in good agreement with our observations: the conductance increased during the first 50 ms and then reached its maximum state where it remained stable for a few to 104 ms. A higher applied field seems to make this state more extended in time. Teruel and Meyer (1997) also have reported that small pores are formed initially, but only a few pores expanded locally to create entry sites large enough for macromolecules to pass. The latter stage occurred over milliseconds. The rate of mass transport is dependent on the concentration gradient and the electric-field gradient across the cell membrane. Both of these factors can be controlled by varying the applied voltage and the concentration of the analyte outside the cell. The membrane was clamped at −50 mV, and, when electropermeabilized inward currents were observed that were reversed at +10 mV, indicating some sort of selection between ions. Because of the delay between application of the electric pulse and formation of pores, the applied field does not affect directly the transport of ions over the membrane. This explanation is consistent with the results presented by Neumann et al. (1998).

Recovery of the membrane usually occurs within 0.5–1 s. The recovery process was longer at higher voltages (Table 1). There seemed to be two time constants involved in membrane recovery: a fast recovery process (milliseconds) as mentioned above, which returns the conductance to the approximate prepulse level, but with a noisier baseline, and a slow process (seconds or longer), which returns this low-conductance state into a state with closed pores. Neumann et al., (1998) have reported dye uptake experiments that indicate pore resealing in kinetically resolved steps for mouse B cells, and Benz and Zimmermann (1981) for planar lipid bilayers. The time scale for recovery is also in good agreement with other studies (Chang and Reese, 1990; Glaser et al., 1988; Teruel and Meyer, 1997). Some of the cells were not fully recovered within 5 min, especially those cells that had experienced higher fields, which indicates that some of the pores have remained stable over minutes. This observation agrees with previous reports, in which pores were

shown to be stable over minutes to hours (Chernomordik et al., 1987; Kinosita and Tsong, 1977a; Lopez et al., 1988).

In the field of biophysical and bioanalytical sciences, a tremendous development toward single-cell- and single-organelle-based technologies has emerged. Our electroporation technique describes the ability to load substances, such as genes, dyes, and pharmaceuticals into single selected cells in a confluent cell culture. This represents, to our knowledge, the highest spatial resolution offered for electroporation and provides, in combination with patch clamp, the opportunity for detailed kinetic and mechanistic studies. This microelectrode system can be developed further for altering the biochemical state of subcellular structures such as organelles, for accessing sensing systems, including receptors, ion channels, and enzymes in single-cell biosensor applications, or for drug targeting a specific group of cells in vivo. For these applications, further optimization studies with regards to voltage pulse parameters (e.g., pulse profile, voltage amplitude, pulse time), electrode materials, and electrode design, including topographically complex microelectrodes, are needed.

We are grateful to Susanne Orwar for digital image editing and photographic work. This work was made possible through grants by the Swedish Natural Science Research Council (grants 10481-305, 308, 309), the Swedish Foundation for Engineering Sciences, the Swedish Foundation for Strategic Research, and The Swedish Foundation for International Cooperation in Research and Higher Education (STINT) for a visiting scientist scholarship to D.T.C.

REFERENCES

Benz, R., and U. Zimmermann. 1980. Pulse-length dependence of the electrical breakdown in lipid bilayer membranes. *Biochim. Biophys. Acta.* 597:637–642.

Benz, R., and U. Zimmermann. 1981. The resealing process of lipid bilayers after reversible electrical breakdown. *Biochim. Biophys. Acta.* 640:169–178.

Bliss, J. G., G. I. Harrison, J. R. Mourant, K. T. Powell, and J. C. Weaver. 1988. Electroporation: the distribution of macromolecular uptake and shape changes in red blood cells following a single 50 msecond square wave pulse. *Bioelectrochem. Bioenerg.* 19:57–71.

Capecchi, M. R. 1980. High efficiency transformation by direct microinjection of DNA into cultured mammalian cells. *Cell.* 22:479–488.

Chang, D. C. 1989. Cell poration and cell fusion using an oscillating electric field. *Biophys. J.* 56:641–652.

Chang, D. C., and T. S. Reese. 1990. Changes in membrane structure induced by electroporation as revealed by rapid-freezing electron microscopy. *Biophys. J.* 58:1–12.

Chernomordik, L. V., S. I. Sukharev, S. V. Popov, V. F. Pastushenko, A. V. Sokirko, I. G. Abidor, and Y. A. Chizmadzhev. 1987. The electrical breakdown of cell and lipid membranes: the similarity of phenomenologies. *Biochim. Biophys. Acta.* 902:360–373.

Chiu, D. T., S. J. Lillard, R. H. Scheller, R. N. Zare, S. E. Rodriguez-Cruz, E. R. Williams, O. Orwar, M. Sandberg, and J. A. Lundqvist. 1998. Probing single secretory vesicles with capillary electrophoresis. *Science.* 279:1190–1193.

Chow, R. H., L. von Ruden, and E. Neher. 1992. Delay in vesicle fusion revealed by electrochemical monitoring of single secretory events in adrenal chromaffin cells. *Nature.* 356:60–63.

Gift, E. A., and J. C. Weaver. 1995. Observation of extremely heterogeneous electroporative uptake which changes with electric field pulse amplitude in *Saccharomyces cerevisiae. Biochim. Biophys. Acta.* 1234: 52–62.

Glaser, R. W., S. L. Leikin, L. V. Chernomordik, V. F. Pastushenko, and A. I. Sokiro. 1988. Reversible electrical breakdown of lipid bilayers: formation and evolution of pores. *Biochim. Biophys. Acta.* 940:275–287.

Hamill, O. P., A. Marty, E. Neher, B. Sakmann, and F. J. Sigworth. 1981. Improved patch-clamp techniques for high-resolution current recording from cells and cell-free membrane patches. *Pflügers Arch.* 391:85–100.

Hibino, M., M. Shigemori, H. Itoh, K. Nagayama, and K. Kinosita, Jr. 1991. Membrane conductance of an electroporated cell analyzed by submicrosecond imaging of transmembrane potential. *Biophys. J.* 59: 209–220.

Kinosita, K., Jr., I. Ashikawa, N. Saita, H. Yoshimura, H. Itoh, K. Nagayama, and A. Ikegami. 1988. Electroporation of cell membrane visualized under a pulsed-laser fluorescence microscope. *J. Biophys.* 53: 1015–1019.

Kinosita, K., Jr., and T. Y. Tsong. 1977a. Voltage-induced pore formation and haemolysis of human erythrocytes. *Biochim. Biophys. Acta.* 471: 227–242.

Kinosita, K., Jr., and T. Y. Tsong. 1977b. Formation and resealing of pores of controlled sizes in human erythrocyte membrane. *Nature.* 268: 438–441.

Kinosita, K., Jr., and T. Y. Tsong. 1979. Voltage-induced conductance in human erythrocyte membranes. *Biochim. Biophys. Acta.* 554:479–497.

Lopez, A., M. P. Rols, and J. Teissié. 1988. P NMR analysis of membrane phospholipid organization in viable, reversibly electropermeabilized Chinese hamster ovary cells. *Biochemistry.* 27:1222–1228.

Lundqvist, J. A., F. Sahlin, M. A. I. Åberg, A. Strömberg, P. S. Eriksson, and O. Orwar. 1998. Altering the biochemical state of individual cultured cells and organelles with ultramicroelectrodes. *Proc. Natl. Acad. Sci. USA.* 95:10356–10360.

Maiti, S., J. B. Shear, R. M. Williams, W. R. Zipfel, and W. W. Webb. 1997. Measuring serotonin distribution in live cells with three-photon excitation. *Science.* 275:530–532.

Marszalek, P. E., B. Farrel, P. Verdugo, and J. M. Fernandez. 1997. Kinetics of release of serotonin from isolated secretory granules. I. Amperometric detection of serotonin from electroporated granules. *Biophys. J.* 73:1160–1168.

Neumann, E., K. Toensing, S. Kakorin, P. Budde, and J. Frey. 1998. Mechanism of electroporative dye uptake by mouse B cells. *Biophys. J.* 74:98–108.

O'Neill, R. J., and L. Tung. 1991. Cell-attached patch clamp study of the electropermeabilization of amphibian cardiac cells. *Biophys. J.* 59: 1028–1039.

Owen, D. G., and M. R. C. Piotrowski. 1987. Electropermeabilization of single cells under patch clamp. *J. Physiol.* 390:14.

Pliquett, U., E. A. Gift, and J. C. Weaver. 1996. Determination of the electric field and anomalous heating caused by exponential pulses in electroporation experiments. *Bioelectrochem. Bioenerg.* 39:39–53.

Pliquett, U., R. Langer, and J. C. Weaver. 1995. Changes in the passive electrical properties of human stratum corneum due to electroporation. *Biochim. Biophys. Acta.* 1239:111–121.

Pliquett, U., and J. C. Weaver. 1996. Electroporation of human skin: simultaneous measurement of changes in the transport of two fluorescent molecules and in the passive electrical properties. *Bioelectrochem. Bioenerg.* 39:1–12.

Prausnitz, M. R., V. G. Bose, R. Langer, and J. C. Weaver. 1993. Electroporation of mammalian skin: a mechanism to enhance transdermal drug delivery. *Proc. Natl. Acad. Sci. USA.* 90:10504–10508.

Sharma, V., K. Stebe, J. C. Murphy, and L. Tung. 1996. Poloxamer 188 decreases susceptibility of artificial lipid membranes to electroporation. *Biophys. J.* 71:3229–3241.

Song, A., S. Parus, and R. Kopelman. 1997. High-performance fiber-optic pH microsensors for practical physiological measurements using a dual-emission sensitive dye. *Anal. Chem.* 69:863–867

Strömberg, A., F. Ryttsén, D. T. Chiu, M. Davidson, P. S. Eriksson, C. F. Wilson, O. Orwar, and R. N. Zare. 2000. Manipulating the genetic identity and biochemical surface properties of individual cells with electric-field-induced fusion. *Proc. Natl. Acad. Sci. USA.* 97:7–11.

Teissié, J., and M.-P. Rols. 1993. An experimental evaluation of the critical potential difference inducing cell membrane electropermeabilization. *Biophys. J.* 65:409–413.

Teissié, J., and T. Y. Tsong. 1981. Electric field induced transient pores in phospholipid bilayer vesicles. *Biochemistry.* 20:1548–1554.

Teruel, M. N., and T. Meyer. 1997. Electroporation-induced formation of individual calcium entry sites in the cell body and processes of adherent cells. *Biophys. J.* 73:1785–1796.

Weaver, J. C. 1993. Electroporation: a general phenomenon for manipulating cells and tissues. *J. Cell. Biochem.* 51:426–435.

Weaver, J. C., and Y. A. Chizmadzhev. 1996. Theory of electroporation: a review. *Bioelectrochem. Bioenerg.* 41:135–160.

Wightman, R. M., J. A. Jankowski, R. T. Kennedy, K. T. Kawagoe, T. J. Scroeder, D. J. Leszczyszyn, J. A. Near, E. J. Diliberto, Jr., and O. H. Viveros. 1991. Temporally resolved cathecholamine spikes correspond to single vesicle release from individual chromaffin cells. *Proc. Natl. Acad. Sci. USA.* 88:10754–10758.

Wilhelm, C., M. Winterhalter, U. Zimmermann, and R. Benz. 1993. Kinetics of pore size during irreversible electrical breakdown of lipid bilayer membranes *Biophys. J.* 64:121–128.

Zheng, Q. A., and D. C. Chang. 1991. High-efficiency gene transfection by in situ electroporation of cultured cells. *Biochim. Biophys. Acta.* 1088: 104–110.

Zimmerman, U. 1982. Electric field-mediated fusion and related electrical phenomena. *Biochim. Biophys. Acta.* 694:227–277.

Zimmermann, U., G. Pilwat, and F. Riemann. 1974. Dielectric breakdown of cell membranes. *Biophys. J.* 14:881–899.